Inorganic Chemistry

Article

pubs.acs.org/IC

Ligand Induced Anionic Cuprous Cyanide Framework for Cupric Ion Turn on Luminescence Sensing and Photocatalytic Degradation of Organic Dyes

Xiao-Yan Xu, Qiu-Cheng Chen, Ya-Dong Yu, and Xiao-Chun Huang*

Department of Chemistry and Key Laboratory for Preparation and Application of Ordered Structural Materials of Guangdong Province, Shantou University, Shantou 515063, China

Supporting Information

ABSTRACT: A new microporous luminescent coordination polymer $[(CH_3)_2NH_2]\cdot[Cu_2(CN)_3]$ (**1**) with channels occupied by dimethylamine cations was synthesized due to the inducing effect of 2-(2′-pyridyl)imidazole. Complex **1** exhibits bright-green emission in the solid state, and its emission intensity would be significantly enhanced, especially by DMAc and cupric ion after immersing the as-synthesized crystals of **1** into common organic solvents or methanol solutions of various metal ions. In addition, **1** exhibits photocatalytic activity for the degradation of RhB and MB under natural light and is stable during the photocatalysis process. Thus, **1** can act as a multifunctional material for selectively sensing of Cu^{2+} and effectively photocatalytic degradation of dyes.

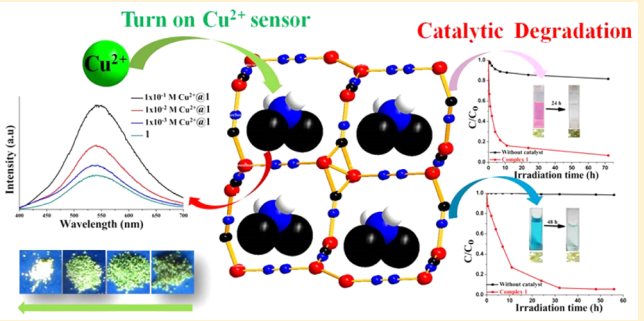

INTRODUCTION

Over the past few decades, cyanide-bridged metal coordination polymers have received increasing attention due to their various structures and intriguing magnetic,[1] porous,[2] and luminescent properties,[3] through the judicious choice of metal centers as well as bridging or ancillary ligands.[4] In terms of structural diversity, cyanide-bridged metal coordination polymers have diverse structures such as single or double chains, sheets and 3D frameworks owing to variable coordination modes of cyanide, as shown in Scheme 1.[5−7] In contrast to numerous 3D microporous coordination polymers without involving cyanide being extensively studied,[8−10] the reported examples of 3D cuprous cyanide open frameworks are still rare mainly because cyanide often chooses the first three coordination modes, and hence generates low-dimensional structures. Recently, Zhang etc. reported several 3D cuprous cyanide open frameworks based on $Cu_2(CN)_6$ building unit in which two bridged cyanides adopt the fourth type μ_3-C,C,N mode (Scheme 1).[11] However, further applications of these cyanide compounds have not been investigated.

Scheme 1. Bridging Modes of Metal−Cyano Complexes

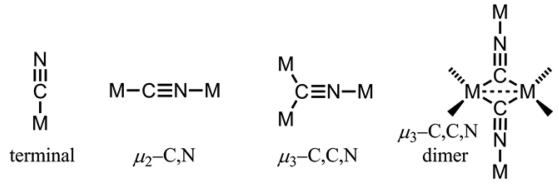

More recently, the design of chemical sensors for small molecules and ions has become a hot topic in the research area of coordination polymer materials,[12−14] because these target analytes play a crucial role in chemical, biological, and environmental processes.[15] Among various cations, sensing for Cu^{2+} is very important, because Cu^{2+} is one of the most essential and important ions in living biological systems,[16] particularly in the brain. For instance, excess amount of Cu^{2+} would disturb the cellular homeostasis, leading to some neurodegenerative and metabolism disorders like Alzheimer's disease and Wilson's disease.[17] Currently, fluorescence detection techniques have become powerful tools for sensing and imaging trace amounts of Cu^{2+} because of their simplicity, sensitivity, and real-time monitoring in short response time.[18] It is well-known that Cu^{2+} usually acts as a fluorescence quencher due to its paramagnetic nature which would lead to a radiationless energy or charge transfer process.[19] Nevertheless, few organics containing CN^- or S have been reported for sensing Cu^{2+} based on fluorescence enhancement, which are subject to the photoinduced electron transfer (PET) mechanism.[20] The metal coordination polymers, which possess better stability, recyclability as well as less pollution, have not been reported yet for sensing Cu^{2+} via fluorescence enhancement. Therefore, it is very meaningful and important to develop stable metal coordination polymers as turn on fluorescent sensors to detecting Cu^{2+}.

Received: August 10, 2015

DOI: 10.1021/acs.inorgchem.5b01820
Inorg. Chem. XXXX, XXX, XXX−XXX

In this work, we report the synthesis and structural characterization of two anionic cuprous cyanide coordination polymer, namely $[(CH_3)_2NH_2]\cdot[Cu_2(CN)_3]$ (**1**) and $[(CH_3)_2NH_2]\cdot[Cu_3(CN)_4]$ (**2**). **1** is a 3D anionic cuprous cyanide coordination polymer synthesized under the induction of 2-(2′-pyridyl)imidazole, whereas **2** would be obtained in the absence of induced ligand. The framework of **1** contains 1D channels occupied by the cationic guest $NH_2Me_2^+$ (dimethylammonium, DMA)), which can selectively exchange with Cu^{2+} ions and exhibits enhanced luminescence properties. Moreover, **1** can also show photocatalytic degradation for rhodamine B (RhB) and methylene blue (MB) because of the low band gap energy. To the best of our knowledge, such multifunctional coordination polymer with a simple cuprous cyanide framework has not been reported for photocatalytic degradation of organic dye, and selectively sensing Cu^{2+} based on luminescence enhancement.

EXPERIMENTAL SECTION

Materials and Measurements. The ligand 2-(2′-pyridyl)imidazole (PyHim) was synthesized according to the literature (Figure S1).[21] CuCN, methanol, and DMF were obtained from commercial sources, and were used as received without further purification. The phase purity of target product was confirmed by powder X-ray diffraction (PXRD) using a D8 Advance X-ray diffractometer. Infrared spectra were recorded on a Nicolet Avatar 360 FTIR spectrophotometer as KBr pellets in the 4000−400 cm^{-1} region. Elemental analyses of C, H, and N were determined using an Elementar Vario EL cube CHNS analyzer. Thermogravimetric analyses (TGA) were performed by heating the crystalline sample from 30 to 800 °C at a rate of 10 °C min^{-1} under nitrogen gas flow on Netzsch STA 449C equipment. Solid UV−vis diffuse reflectance spectra were measured with a Lambda 950 UV/vis Spectrometer. Inductively Coupled Plasma-atomic Emission Spectrometry (ICPE-9000) was used to measure the content of metal in the sample. Steady-state photoluminescence spectra were measured by a single-photon counting spectrometer using an Edinburgh FLS920 spectrometer equipped with a continuous Xe900 xenon lamp.

Synthesis. $[(CH_3)_2NH_2]\cdot[Cu_2(CN)_3]$ (1). A mixture of CuCN (0.0447 g, 0.50 mmol), PyHim (0.0302 g, 0.20 mmol), MeOH (5 mL), and DMF (5 mL) was sealed in a 15 mL Teflon-lined stainless container and heated to 140 °C for 72 h, and then cooling to room temperature at a rate of 5 °C h^{-1}. The light yellow crystals of **1** in yield of 45% were obtained based on CuCN.

$[(CH_3)_2NH_2]\cdot[Cu_3(CN)_4]$ (2). The synthetic procedure of **2** is similar to that of **1** except for the absence of PyHim. The light yellow crystals of **2** in yield of less than 10% were obtained based on CuCN.

X-ray Crystallography. Single crystals of **1** and **2** were carefully selected under an optical microscope and glued to thin glass fibers. Structural measurements were performed on a computer-controlled Siemens Smart CCD diffractometer with graphite-monochromatic Mo *Kα* radiation (λ = 0.710 73 Å) at 295 K. Absorption corrections were applied by using the multicar program SADABS. Structural solutions and full-matrix least-squares refinements based on F^2 were performed with the SHELX-97 program packages. Anisotropic thermal parameters were applied to all non-hydrogen atoms. All the hydrogen atoms were generated geometrically. The selected crystal parameters, data collection, and refinements are summarized in Table 1. Selected bond lengths and bond angles are given in Tables S1−S4.

RESULTS AND DISCUSSION

Crystal Structure Description. X-ray crystal structure analysis reveals that complex **1** crystallizes in the monoclinic space group $P2_1/c$, and the asymmetric unit contains two crystallographically independent copper centers, three cyanides, and one protonated dimethylamine cation as shown in Figure 1a. The atoms C3/N3 and C4/N4 from half cyanide present site occupancy disorder with the same site occupancy 0.5, respectively. Cu1 center displays a tetrahedral geometry, coordinated by four carbon and/or nitrogen atoms from four cyanides. The Cu1—X (X = C or N) bond lengths are in the range of 1.937(5)−2.143(5) Å, and the X—Cu1—X bond angles span the range of 107.2(2)−118.5(2) °. Cu2 center shows a triangle coordination geometry, coordinated by three carbon and/or nitrogen atoms from three cyanides. The Cu1—C/N bond lengths are in the range of 1.898(5)−2.143(5) Å, and the X—Cu1—X bond angles span the range of 116.8(3)−123.1(2) °. The cyanides are coordinated to Cu(I) atoms in μ_2-C,N and μ_3-C,C,N modes, respectively. Complex **1** contains 2D layered $[Cu_4(CN)_5]^-$ motifs which are formed by fusion of $[Cu_5(CN)_5]$ rings (Figure 1b). These 2D layers are further connected by cyanides to form a 3D microporous framework. Along the *a*, *b*, and *c* directions, **1** exhibits three types of 1D open channels, with the size of ca. 3.9 × 4.4 $Å^2$ (Figure 1c), 6.2 × 6.5 $Å^2$ and 4.0 × 7.2 $Å^2$, respectively (Figure S2, measured between opposite atoms and van der Waals radii of the atoms are take into account). According to the charge balance and element analysis, the framework is anionic with protonated dimethylamine cations residing in the channel along the *a*-axis direction (Figure 1c). In addition, **1** could be considered to be built by six-connected $Cu_2(CN)_6$ and three-connected $Cu(CN)_3$ SBUs, forming an 3D (3,6)-connected **mcn** net as shown in Figure 1d.

Table 1. Crystallographic Data for 1 and 2

compound	1	2
formula	$C_5H_8Cu_2N_4$	$C_6H_8Cu_3N_5$
F_w	251.23	340.79
crystal system	monoclinic	monoclinic
space group	$P2_1/c$	$I2/a$
a, Å	6.5653(2)	12.442(1)
b, Å	14.1231(6)	8.5818(4)
c, Å	12.6927(4)	12.4877(7)
ß, deg	91.462(4)	105.143(6)
V, $Å^3$	1176.5(7)	1287.0(1)
Z	4	4
D_c, mg·mm^{-3}	1.418	1.759
μ, mm^{-1}	3.570	4.883
reflns collected/unique	5628/2064	2064/998
GOF on F^2	1.061	1.050
R_1[a] ($I > 2\sigma(I)$)	0.0457	0.0473
wR_2[b] (all data)	0.1535	0.1349

[a] $R_1 = \sum||F_0| - |F_c||/\sum|F_0|$; $wR_2 = \{[\sum w(F_0^2 - F_c^2)^2]/\sum[w(F_0^2)^2]\}^{1/2}$. [b] $w = 1/[\sigma^2(F_0^2) + (aP)^2 + bP]$, where $P = [\max(F_0^2, 0) + 2F_c^2]/3$ for all data.

Complex **2** crystallizes in the monoclinic space group $I2/a$, and the asymmetric unit contains one and half crystallographically independent copper centers, two cyanides, and half protonated dimethylamine cation as shown in Figure 2a. The atoms of Cu2, N3, C3, and C4 are located in the special positions with site occupancy of 0.5. Cu1 center shows a triangle geometry, coordinated by C1, N1A, and N2 atoms. The Cu1—C bond lengths are 1.916(6) Å, and the Cu1—N bond lengths are 1.956(6) and 1.961(8) Å. The C—Cu1—N bond angles are in the range of 119.8(3)−122.2(2)°. The Cu2 atom shows a linear coordination geometry, coordinated by two C2 atoms. The Cu2—C bond length is 1.916(6) Å. Complex **2** is found to be a 2D layered network based on $[Cu_8(CN)_8]$

DOI: 10.1021/acs.inorgchem.5b01820
Inorg. Chem. XXXX, XXX, XXX−XXX

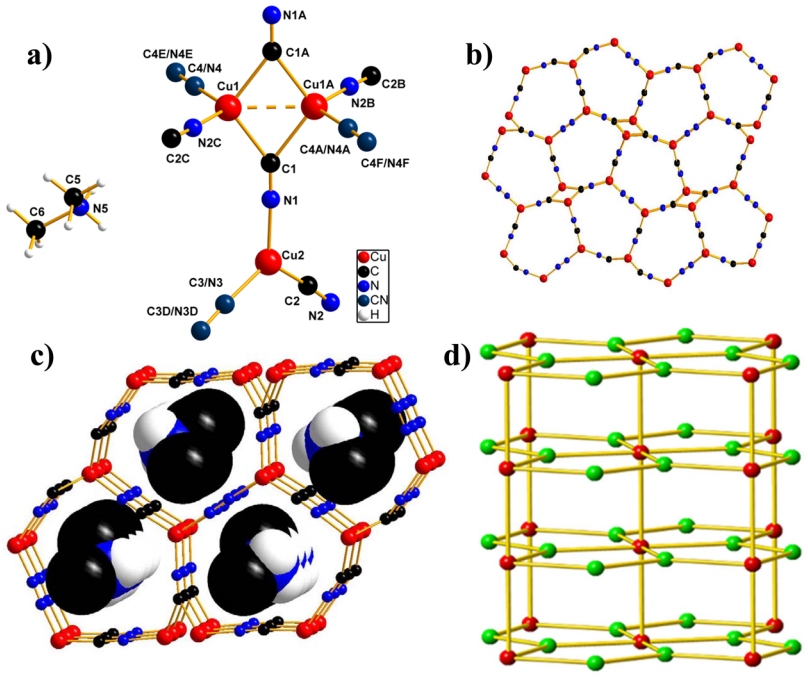

Figure 1. (a) The coordination environments of copper atoms in **1**; (b) 2D $[Cu_4(CN)_5]^-$ layer constructed by $[Cu_5(CN)_5]$ rings in **1**; (c) 3D microporous framework of **1** with dimethylamine cations shown in space-filling mode along *a*-axis; and (d) the topology representation of **1**.

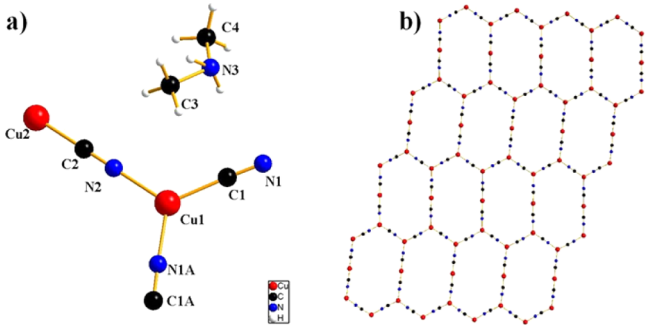

Figure 2. (a) The coordination environments of copper atoms in **2** and (b) 2D $[Cu_3(CN)_4]^-$ layer constructed by $[Cu_8(CN)_8]$ rings in **2**.

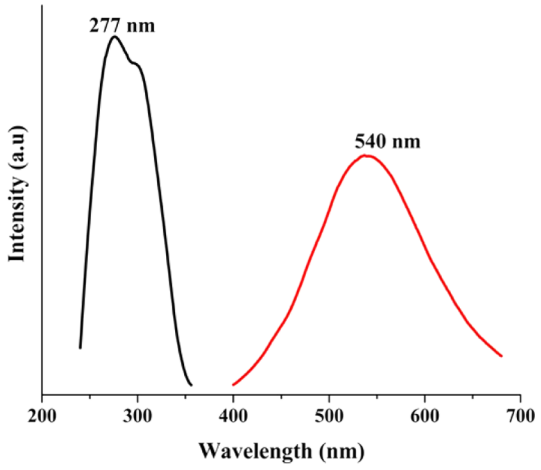

Figure 3. Solid state excitation (black, λ_{em} = 540 nm) and emission (red, λ_{ex} = 277 nm) spectra of **1**.

rings (Figure 2b). According to the charge balance and element analysis, the framework is anionic with protonated dimethylamine cations filling the empty space.

Synthesis and Thermal Stability. It is well-known that the construction of open frameworks under solvothermal conditions is easily affected by various factors, and a slight change such as different metal ions, additives, templates, solvents, and reaction temperatures, may result in different products.[22,23] **1** was solvothermally obtained by treatment of CuCN, MeOH, DMF and PyHim, while similar procedures were employed for the preparation of **2** except for the absence of PyHim. Although PyHim is not incorporated in the final as-made product **1**, it may induce the formation of the 3D framework. Besides, at different reaction temperatures such as 160 °C, 120 °C, and 90 °C, similar reactions could not give crystalline products. Due to poor yield of **2**, the properties determination was focused on complex **1**.

Thermogravimetric analysis for **1** was performed on a polycrystalline sample (Figure S3), which shows that almost no weight loss occurred until 200 °C, indicating good thermal stability of **1**, and then framework decomposes upon further heating, with ca. 58% weight loss during 203−400 °C corresponding to removal of dimethylamine cations and ligands.

Photoluminescence. Complex **1** shows a strong green emission with maximum emission band at 540 nm with 277 nm excitation in the solid state at room temperature (Figure 3). The emission of **1** may be assigned to metal-to-ligand charge transfer wherein the charge is transferred from Cu(I) to π^* orbital of cyanide group,[24] and Cu-centered transitions (MC).[25] In addition, the partial contribution of Cu—Cu bonding cannot be ruled out, because **1** has a short Cu···Cu distance (2.4925(1) Å).[26]

Qualitative Sensing of Solvents. The photoluminescence (PL) properties of **1** after immersing the as-synthesized sample into various solvents for 24 h were measured (Figure 4).

DOI: 10.1021/acs.inorgchem.5b01820
Inorg. Chem. XXXX, XXX, XXX−XXX

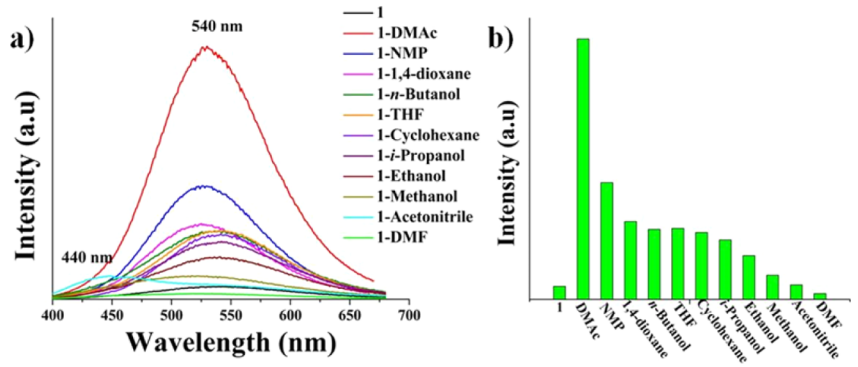

Figure 4. (a) The solid state PL spectra and (b) the relative emission intensity of **1** after immersing the as-synthesized sample into various pure solvents when excited at 277 nm.

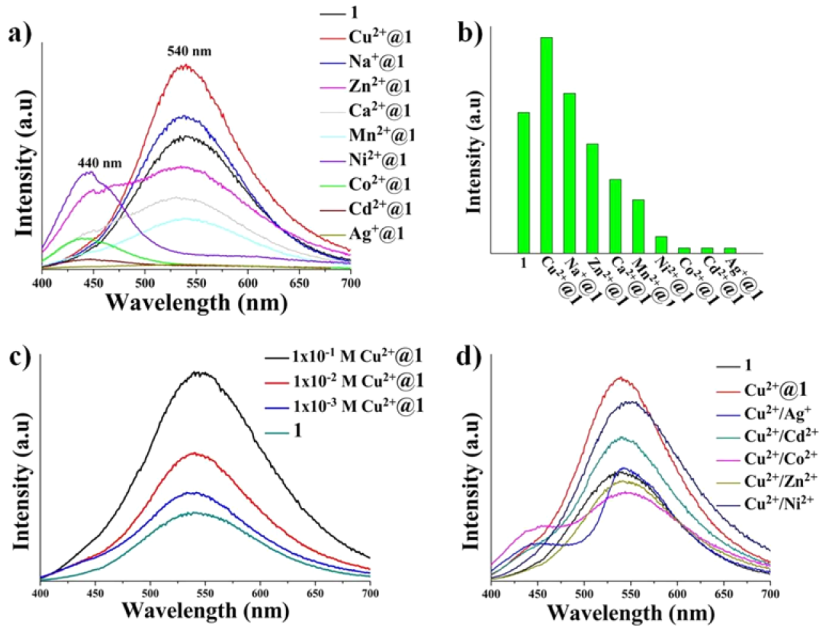

Figure 5. Solid state PL spectra (a) and relative emission intensity (b) of **1** after immersing the as-synthesized sample into methanol solution with various metal ions (0.01 M) for 5 days when excited at 277 nm; (c) the solid state PL spectra of **1** after immersing the as-synthesized sample into methanol solution with different concentrations of Cu^{2+} (λ_{ex} = 277 nm); and (d) the solid state PL spectra of **1** after immersing the as-synthesized sample into methanol solution with binary metal ions (0.01 M, 1:1, Cu^{2+}/M^{x+}, M^{x+} = Zn^{2+}, Cd^{2+}, Co^{2+}, Ni^{2+}, and Ag^{+}) for 5 days when excited at 277 nm.

Interestingly, the spectra are dependent on the solvent molecules with obvious change of emission intensity and energy (Figure 4a). Particularly, DMAc and DMF bearing similar structure and polarity show the opposite effect, displaying the greatest enhancing and slightly quenching effect, respectively (Figure 4b). Furthermore, **1** gives priority to sense DMAc in mixed solutions of DMF and DMAc, which is easily detected by the naked eyes upon UV excitation (Figure S4). Another distinctive case is acetonitrile which shows a blue-shifted emission maximum at λ = 440 nm while the original emission of **1** exhibits emission with λ_{max} = 540 nm. According to PXRD measurement (Figure S5), it is found that the framework of **1** after immersing into DMAc, DMF and the mixed solution of DMF and DMAc are still stable, while the framework of **1** after being immersed into acetonitrile is destroyed or transformed to another crystalline phase, which may lead to a blue shift of the emission band. One possible explanation for the luminescence enhanced phenomenon could be that the proton may transfer between the solvent molecules and dimethylamine cations, or the solvent molecules directly enter into the pores in **1**, which may have an impact on the charge transfer process from Cu(I) centers to π^* orbital of cyanide groups.[27]

Cations Sensing Properties. To explore the potential capacity of **1** for sensing metal ions, the as-synthesized sample was immersed into methanol solution containing 0.01 M $M(NO_3)_x$ (M^{x+} = Na^+, Ag^+, Ca^{2+}, Mn^{2+}, Ni^{2+}, Co^{2+}, Cu^{2+}, Zn^{2+}, or Cd^{2+}, respectively) for 5 days to form M^{x+}@**1** as crystalline solids for luminescence sensing studies. The photoluminescence properties of M^{x+}@**1** are recorded and compared in Figure 5a,b, where only Cu^{2+} and Na^+ enhance the emission while the rest quench the emission at different degrees. For Ni^{2+}@**1**, Co^{2+}@**1** and Cd^{2+}@**1**, a new emission band at 440 nm is generated and the original emission of **1** at 540 nm disappears. Zn^{2+}@**1** and Ca^{2+}@**1** generate a new shoulder at 440 nm and the emission band at 540 nm still exists. Ag^+@**1** shows the most significant quenching effect. Surprisingly, Cu^{2+} gives the strongest luminescent enhanced effect. It is well-

DOI: 10.1021/acs.inorgchem.5b01820
Inorg. Chem. XXXX, XXX, XXX−XXX

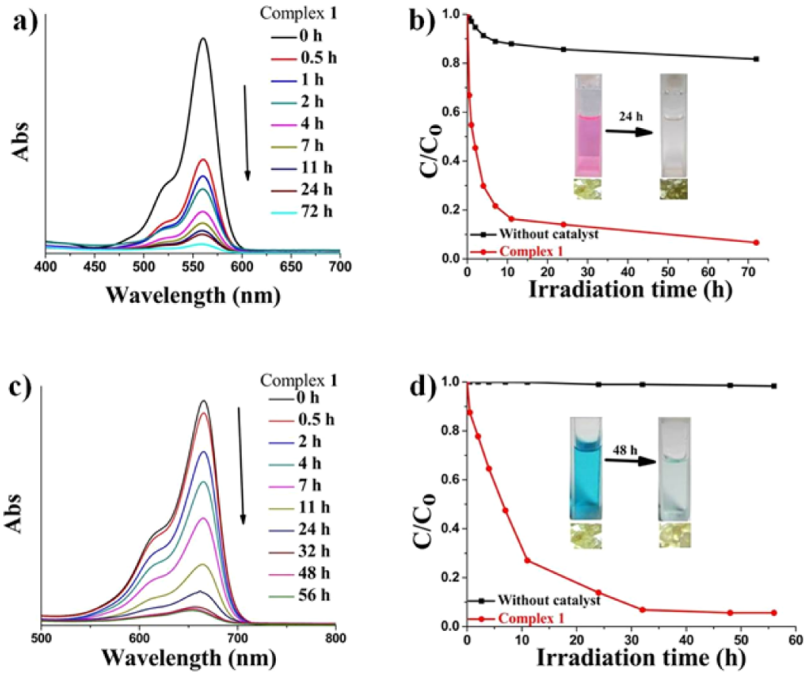

Figure 6. (a) Absorption spectra of the RhB solution during the degradation reaction under natural light with the presence of **1**; (b) time-dependent concentration changes of RhB solution with **1** (red line) and without catalyst in the same conditions (black line), insert: photographs showing the color change of RhB solution and the crystalline samples of **1** after degradation for 24 h; (c) absorption spectra of the MB solution during the degradation reaction in natural light with the presence of **1**; and (d) time-dependent concentration changes of MB solution with **1** (red line) and without catalyst in the same conditions (black line), insert: photographs showing the color change of MB solution and the crystalline samples of **1** after degradation for 48 h.

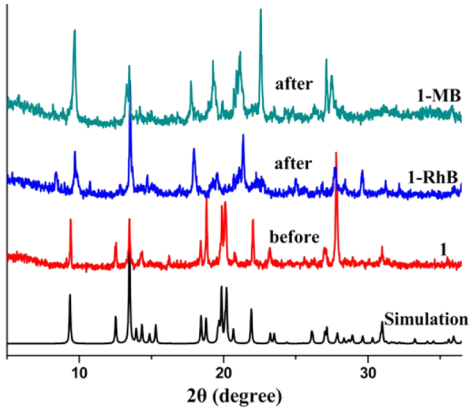

Figure 7. PXRD patterns of **1** before and after the degradation process of RhB and MB, respectively.

known that the luminescence quenching effect by metal ions acting on coordination polymers generally originating three ways: (i) the ions exchange between central metal ions of coordination polymers and the targeted ions;[28] (ii) the collapse of the crystal structure;[29] and (iii) the interaction between metal ions and organic ligands.[30] According to PXRD patterns (Figure S6), it is found that the diffraction peaks of Cd^{2+}@**1**, Co^{2+}@**1**, Ni^{2+}@**1**, and Ag^{+}@**1** do not correspond to those of **1**, indicating the frameworks may be destroyed, whereas Zn^{2+}@**1** and Cu^{2+}@**1** possess almost the same diffraction peaks with those of **1**, showing that these ions only slight affect the framework of **1**. In addition, it is found that the Cu^{2+} content of Cd^{2+}@**1**, Co^{2+}@**1**, Ni^{2+}@**1**, Zn^{2+}@**1**, and Ag^{+}@**1** are less than that of **1**, and the existence of these cations are detected simultaneously through the ICP analysis (Table S5), which suggests that the Cd^{2+}, Co^{2+}, Ni^{2+}, Zn^{2+}, and Ag^{+} may partly exchange with both $[(CH_3)_2NH_2]^{+}$ and central Cu^{+} in **1**. On

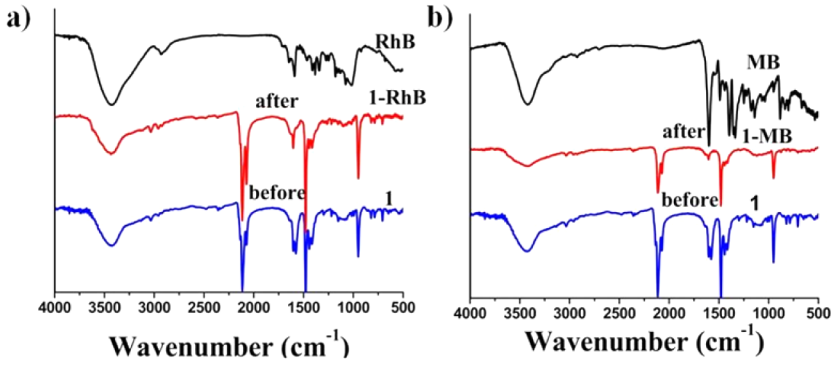

Figure 8. IR spectra of **1** before (a) and after (b) the degradation process of RhB and MB, respectively.

DOI: 10.1021/acs.inorgchem.5b01820
Inorg. Chem. XXXX, XXX, XXX−XXX

the basis of the above analysis, it can be speculated that the collapse of the crystal structure of Cd^{2+}@**1**, Co^{2+}@**1**, Ni^{2+}@**1**, and Ag^{+}@**1** in different degrees result in the quenching effect and blue shifts of the photoluminescence spectra.

Given the interesting luminescence enhanced effect of Cu^{2+} on **1**, the further study was carried out. First, with the increasing concentration of Cu^{2+}, the emission intensity of **1** is greatly enhanced (Figure 5c), which is easily detected by the naked eye upon UV excitation (Figure S7). Second, the content of copper was detected by ICP (Table S6) which gives 54.5% (mass percent) for 10^{-3} M Cu^{2+}@**1** and 70.8% for 10^{-2} M Cu^{2+}@**1**, respectively, compared to 48.9% for as-synthesized **1**. It should be mentioned that the crystal frameworks keep unchanged when immersed into the lower concentration (0.001 and 0.01 M) Cu^{2+} solutions, but higher concentration Cu^{2+} (0.1 M) will greatly destroy the crystallinity according to the PXRD patterns (Figure S8). In addition, according to elemental analysis (Table S7), it is found that the N contents of Cu^{2+}@**1** decrease with the increasing concentration of cupric ion. On the basis of the above investigations, cupric ions should enter into the channel with exchanging some guest cations $[(CH_3)_2NH_2]^+$ in **1**. However, there is still a crucial problem being not addressed, that is why cupric ions into the pores will lead to the enhanced luminescence. Tian and co-workers[31] recently reported a work in which new unsymmetrical diarylethenes were synthesized, and the addition of cupric ions would result in the enhanced luminescence. Furthermore, when cyanides were added into the Cu^{2+} postsynthesized system, the emission was further enhanced. In our work, the interactions between cupric ions and framework were confirmed by IR which shows that the C≡N stretching vibration peak has blue shift from 2112 to 2167 cm^{-1} (Figure S9) after being immersed into Cu^{2+} solution. The strong binding tendency of cupric ion toward C≡N group should be responsible for the enhanced luminescence effect. In order to get further insight into this luminescence enhanced phenomenon, the CuCN powder sample was immersed into 0.01 M $Cu(NO_3)_2$ solution and $Zn(NO_3)_2$ for 5 days, respectively, then the postsynthesized M^{x+}−CuCN solids were used for luminescence study. The photoluminescence properties of M^{x+}−CuCN are recorded in Figure S10. The surprising result is that Cu^{2+} also shows the greatest enhancing luminescence for CuCN, while Zn^{2+} does not. It suggests that Cu^{2+} may favor the photoluminescence of compounds bearing C≡N group due to the strong binding tendency of cupric ion toward C≡N group.

Since the luminescence intensity of M^{x+}@**1** is dependent on the nature of metal ions, it provides the possibility to selectively sense Cu^{2+}. In the binary Cu^{2+}/M^{x+} systems (M^{x+} = Zn^{2+}, Cd^{2+}, Co^{2+}, Ni^{2+}, and Ag^{+}, Figure 5d), it is found that the Cd^{2+}, Zn^{2+}, and/or Ag^{+} have no effect on the sensing functions of **1** for Cu^{2+}, because there are no blue shift and quenching effects in the photoluminescence (PL) spectra. However, the mixtures of Cu^{2+}/Co^{2+} and Cu^{2+}/Ni^{2+} solution still have some differences with the single Cu^{2+} solution: there are two maximum emissions at 440 and 540 nm, but without quenching effects. According to the ICP test analysis (Table S6), the content of Cu^{2+} in Cu^{2+}/Co^{2+}@**1** and Cu^{2+}/Ni^{2+}@**1** are more than **1**, but the Co^{2+} and Ni^{2+} contents are less than Co^{2+}@**1** and Ni^{2+}@**1**, indicating that the bright potential of compound **1** gives priority to sense for Cu^{2+} in aqueous solution.

Photocatalytic Degradation of Organic Dyes. Some organic dyes are chemically stable and not readily biodegradable in water, which makes them potentially harmful to the ecoenvironment.[32,33] Methylene blue (MB) and rhodamine B (RhB) as typical pollutants in aqueous media, being highly toxic and difficult to degrade, have become one of the most serious global environmental issues today.[34,35] Therefore, an effective and economical technique needs to be developed to reduce the concentration of organic pollutants before releasing the wastewater into the aquatic environment. Recently, photocatalysis is increasingly adopted in the destruction of organic contaminants, due to their high efficiency, simplicity, good reproducibility, and easy handling.[36] Until now, the degradation of organic dyes under natural light is still rare.[37]

The band gap of **1** was determined by the UV−vis diffuse reflection measurement at room temperature and the result gives an E_g (band gap energy) value of 2.40 eV (Figure S11), thus **1** may has the photocatalytic activity for organic dyes.[38] The catalytic performance of **1** for the degradation of methylene blue (MB) and rhodamine B (RhB) was investigated. During the photocatalytic degradation process, 20 mg crystalline samples of **1** was immersed into the RhB (5×10^{-5} mol/L) and MB (1×10^{-5} mol/L) MeOH solution, respectively, then these solutions were placed under natural light and 3.0 mL solution with different degradation time was taken out for UV−vis absorption analysis. As shown in Figure 6, **1** exhibits high photocatalytic efficiency for the degradation of MB, and RhB in aqueous solution under natural light. For the degradation of RhB, the absorption of RhB at about 561 nm was selected to monitor catalytic degradation process. When **1** was dispersed in RhB solution for different time (0−72 h), the degradation rate of RhB reached 91.4% at 24 h and the color of RhB solution changed from red to colorless, as shown in Figure 6a,b. A similar procedure was performed to confirm the catalytic degradation activity of **1** for the degradation of MB. The degradation rate of MB reached 91.8% at 32 h, and the color of MB solution almost completely fades at 48 h, as shown in Figure 6c,d.

After photocatalysis process, the colors of **1** remain unchanged. In addition, the PXRD patterns of the samples used for photocatalytic degradation correspond well to that of as-synthesized **1** (Figure 7), indicating that **1** is stale during the photocatalytic degradation process. Furthermore, from the IR spectra (Figure 8), it is clear that there are no characteristic peaks of RhB and MB in **1** after the photocatalytic degradation process, suggesting that the color fading of RhB and MB are due to photocatalytic degradation, but not being adsorbed into the channels of **1**. On the basis of the above observations, **1** can act as a candidate for the catalytic degradation of RhB and MB under natural light.

In conclusion, we have successfully obtained a novel 3D cuprous cyanide anionic framework with high porosity under solvothermal conditions. Interestingly, **1** exhibits a sensing ability toward various organic solvents and metal cations, especially for DMAc and Cu^{2+} based on a "turn on" manner. Furthermore, **1** displays high efficiency and stability on the photocatalytic degradation of RhB and MB organic dyes under natural light. Therefore, this multifunctional compound may be a good candidate for luminescence probe for Cu^{2+} and photocatalytic degradation of some organic dyes in aqueous solution.

DOI: 10.1021/acs.inorgchem.5b01820
Inorg. Chem. XXXX, XXX, XXX−XXX

■ ASSOCIATED CONTENT

Supporting Information

The Supporting Information is available free of charge on the ACS Publications website at DOI: 10.1021/acs.inorgchem.5b01820.

Structural analysis, TGA, PXRD patterns, solid-state UV photos, PL spectra, The Kubelka−Munk equation transformed UV−vis absorption of **1**, ICP data (PDF)
Elemental analysis data and selected bond lengths and angles for **1** and **2** (CIF)

■ AUTHOR INFORMATION

Corresponding Author

*E-mail: xchuang@stu.edu.cn (X.-C.H.).

Author Contributions

The manuscript was written through contributions of all authors. All authors have given approval to the final version of the manuscript.

Notes

The authors declare no competing financial interest.

■ ACKNOWLEDGMENTS

We gratefully acknowledge financial support from the National Basic Research Program of China (973 Program, 2013CB834803 and 2012CB821700), NSFC (nos. 21171113 and 21571122), and Department of Education in Guangdong Province.

■ REFERENCES

(1) (a) Maxim, C.; Branzea, D. G.; Tiseanu, C.; Rouzieres, M.; Clerac, R.; Andruh, M.; Avarvari, N. *Inorg. Chem.* **2014**, *53*, 2708−2717. (b) Zhou, Y.-L.; Wu, M.-C.; Zeng, M.-H. *Inorg. Chem.* **2009**, *48*, 10146−10150. (c) Clemente-Leoín, M.; Coronado, E.; Martí-Gastaldo, C.; Romero, F. M. *Chem. Soc. Rev.* **2011**, *40*, 473−497.

(2) (a) Zhang, J. P.; Liao, P. Q.; Zhou, H. L.; Lin, R. B.; Chen, X. M. *Chem. Soc. Rev.* **2014**, *43*, 5789−5814. (b) Furukawa, H.; Cordova, K. E.; O'Keeffe, M.; Yaghi, O. M. *Science* **2013**, *341*, 974−986. (c) Herm, Z. R.; Wiers, B. M.; Mason, J. A.; van Baten, J. M.; Hudson, M. R.; Zajdel, P.; Brown, C. M.; Masciocchi, N.; Krishna, R.; Long, J. R. *Science* **2013**, *340*, 960−964.

(3) (a) Rocha, J.; Carlos, L. D.; Paz, F. A.; Ananias, D. *Chem. Soc. Rev.* **2011**, *40*, 926−940. (b) Heine, J.; Muller-Buschbaum, K. *Chem. Soc. Rev.* **2013**, *42*, 9232−9242. (c) Guillerm, V.; Kim, D.; Eubank, J. F.; Luebke, R.; Liu, X.; Adil, K.; Lah, M. S.; Eddaoudi, M. *Chem. Soc. Rev.* **2014**, *43*, 6141−6142. (d) Eddaoudi, M.; Sava, D. F.; Eubank, J. F.; Adil, K.; Guillerm, V. *Chem. Soc. Rev.* **2015**, *44*, 228−249.

(4) (a) Li, Y.; Zhang, S.; Song, D. *Angew. Chem., Int. Ed.* **2013**, *52*, 710−713. (b) Li, X. J.; Jiang, F. L.; Wu, M. Y.; Chen, L.; Qian, J. J.; Zhou, K.; Yuan, D. Q.; Hong, M. C. *Inorg. Chem.* **2014**, *53*, 1032−1038. (c) Handke, M.; Weber, H.; Lange, M.; Mollmer, J.; Lincke, J.; Glaser, R.; Staudt, R.; Krautscheid, H. *Inorg. Chem.* **2014**, *53*, 7599−7607.

(5) (a) Hibble, S. J.; Eversfield, S. G.; Cowley, A. R.; Chippindale, A. M. *Angew. Chem., Int. Ed.* **2004**, *43*, 628−630. (b) Chesnut, D. J.; Kusnetzow, A.; Birge, R.; Zubieta, J. *J. Am. Chem. Soc.* **2001**, 2581−2586.

(6) (a) Liang, S.-W.; Li, M.-X.; Shao, M.; Miao, Z.-X. *Inorg. Chem. Commun.* **2006**, *9*, 1312−1314. (b) Colacio, E.; Domínguez-Vera, J. M.; Lloret, F.; Sánchez, J. M. M.; Kivekäs, R.; Rodríguez, A.; Sillanpää, R. *Inorg. Chem.* **2003**, *42*, 4209−4214.

(7) (a) Amo-Ochoa, P.; Miguel, P. J. S.; Castillo, O.; Zamora, F. *CrystEngComm* **2007**, *9*, 987. (b) Kaase, D.; Gotzmann, C.; Rein, S.; Lan, Y.; Kacprzak, S.; Klingele, J. *Inorg. Chem.* **2014**, *53*, 5546−5555. (c) Zhang, X.-M.; Qing, Y.-L.; Wu, H.-S. *Inorg. Chem.* **2008**, *47*, 2255−2257.

(8) (a) He, Y.-B.; Zhou, W.; Qian, G.-D.; Chen, B.-L. *Chem. Soc. Rev.* **2014**, *43*, 5657−5678. (b) Roy, S.; Chakraborty, A.; Maji, T.-K. *Coord. Chem. Rev.* **2014**, *273*−*274*, 139−164. (c) Qiu, S.-L.; Xue, M.; Zhu, G.-S. *Chem. Soc. Rev.* **2014**, *43*, 6116−6140.

(9) (a) Manna, K.; Zhang, T.; Lin, W.-B. *J. Am. Chem. Soc.* **2014**, *136*, 6566−6569. (b) Xiao, J.; Liu, B.-Y.; Wei, G.; Huang, X.-C. *Inorg. Chem.* **2011**, *50*, 11032−11038. (c) Zeng, M.-H.; Feng, X.-L.; Chen, X.-M. *Dalton Trans.* **2004**, *15*, 2217−2223.

(10) (a) Evans, R. C.; Douglas, P.; Winscom, C. J. *Coord. Chem. Rev.* **2006**, *250*, 2093−2126. (b) Bhattacharyya, S.; Chakraborty, A.; Jayaramulu, K.; Hazra, A.; Maji, T. K. *Chem. Commun.* **2014**, *50*, 13567−13570. (c) Huang, X.-C.; Lin, Y.-Y.; Zhang, J.- P.; Chen, X.- M. *Angew. Chem., Int. Ed.* **2006**, *45*, 1557−1559. (d) Zhang, J.-P.; Zhang, Y.-B.; Lin, J.-B.; Chen, X.-M. *Chem. Rev.* **2012**, *112*, 1001−1033.

(11) Qin, Y.-L; Hou, J.-J.; Lv, J.; Zhang, X.-M. *Cryst. Growth Des.* **2011**, *11*, 3101−3108.

(12) (a) Wang, J.-H.; Li, M.; Li, D. *Chem. Sci.* **2013**, *4*, 1793. (b) Guo, Z.; Xu, H.; Su, S.; Cai, J.; Dang, S.; Xiang, S.; Qian, G.; Zhang, H.; O'Keeffe, M.; Chen, B. *Chem. Commun.* **2011**, *47*, 5551−5553. (c) Shustova, N. B.; Cozzolino, A. F.; Reineke, S.; Baldo, M.; Dinca, M. *J. Am. Chem. Soc.* **2013**, *135*, 13326−13329.

(13) (a) Chen, B.; Wang, L.; Zapata, F.; Qian, G.; Lobkovsky, E. B. *J. Am. Chem. Soc.* **2008**, *130*, 6718−6719. (b) Manna, B.; Singh, S.; Karmakar, A.; Desai, A. V.; Ghosh, S. K. *Inorg. Chem.* **2015**, *54*, 110−116. (c) Karmakar, A.; Manna, B.; Desai, A. V.; Joarder, B.; Ghosh, S. K. *Inorg. Chem.* **2014**, *53*, 12225−12227.

(14) (a) Liu, B.; Wu, W.-P.; Hou, L.; Wang, Y.-Y. *Chem. Commun.* **2014**, *50*, 8731−8734. (b) Hao, J. N.; Yan, B. *Chem. Commun.* **2015**, *51*, 7737−7740. (c) Thakur, A.; Mandal, D.; Deb, P.; Mondal, B.; Ghosh, S. *RSC Adv.* **2014**, *4*, 1918−1928. (d) Cao, J.; Gao, Y.; Wang, Y.; Du, C.; Liu, Z. *Chem. Commun.* **2013**, *49*, 6897−6899.

(15) (a) Martınw, J. C. G.; Plane, J. M. C. *Phys. Chem. Chem. Phys.* **2011**, *13*, 3764−3774. (b) Chanroj, S.; Lu, Y.-X.; Padmanaban, S.; Nanatani, K.; Uozumi, N.; Rao, R.; Sze, H. *J. Biol. Chem.* **2011**, *286*, 33931−33941. (c) Reyes, A. C.; Koudelka, A. P.; Amyes, T. L.; Richard, J. P. *J. Am. Chem. Soc.* **2015**, *137*, 5312−5315. (d) Robinson, N. J.; Winge, D. R. *Annu. Rev. Biochem.* **2010**, *79*, 537−562.

(16) Lelie, H. L.; Liba, A.; Bourassa, M. W.; Chattopadhyay, M.; Chan, P. K.; Gralla, E. B.; Miller, L. M.; Borchelt, D. R.; Valentine, J. S.; Whitelegge, J. P. *J. Biol. Chem.* **2011**, *286*, 2795−2806.

(17) (a) Waggoner, D. J.; Bartnikas, T. B.; Gitlin, J. D. *Neurobiol. Dis.* **1999**, *6*, 221−230. (b) Mercer, J. F.B. *Trends Mol. Med.* **2001**, *7*, 64−70. (c) Cerpa, W.; Varela-Nallar, L.; Reyes, A. E.; Minniti, A. N.; Inestrosa, N. C. *Mol. Aspects Med.* **2005**, *26*, 405−420. (d) Kumar, N.; Low, P. A. *J. Neurol.* **2004**, *251*, 747−749.

(18) (a) Thomas, S. W., III; Joly, G. D.; Swager, T. M. *Chem. Rev.* **2007**, *107*, 1339−1386. (b) Niamnont, N.; Kimpitak, N.; Tumcharern, G.; Rashatasakhon, P.; Sukwattanasinitt, M. *RSC Adv.* **2013**, *3*, 25215−25220. (c) Kar, C.; Adhikari, M. D.; Ramesh, A.; Das, G. *Inorg. Chem.* **2013**, *52*, 743−752. (d) Han, Y.; Ding, C.; Zhou, J.; Tian, Y. *Anal. Chem.* **2015**, *87*, 5333. (e) Liu, J.; Karpus, J.; Wegner, S. V.; Chen, P. R.; He, C. *J. Am. Chem. Soc.* **2013**, *135*, 3144−3149.

(19) Jung, H.- S.; Kwon, P.-S.; Lee, J.- W.; Kim, J.; Hong, C.- S.; Kim, J. W.; Yan, S.; Lee, J.- Y.; Joo, T.; Kim, S. *J. Am. Chem. Soc.* **2009**, *131*, 2008−2012.

(20) (a) Suganya, S.; Velmathi, S.; MubarakAli, D. *Dyes Pigm.* **2014**, *104*, 116−122. (b) Liang, L.-J.; Zhao, L.-C.; Zeng, X.-S. *J. Fluoresc.* **2014**, *24*, 1671−1677.

(21) Voss, M. E.; Beer, C. M.; Mitchell, S. A.; Blomgren, P. A.; Zhichkin, P. E. *Tetrahedron* **2008**, *64*, 645−651.

(22) (a) Yu, J.; Xu, R. *Acc. Chem. Res.* **2010**, *43*, 1195−1204. (b) Perez-Ramirez, J.; Christensen, C. H.; Egeblad, K.; Christensen, C. H.; Groen, J. C. *Chem. Soc. Rev.* **2008**, *37*, 2530−2542.

(23) (a) Chen, X.-M.; Tong, M.-L. *Acc. Chem. Res.* **2007**, *40*, 162−170. (b) Zhang, X.-M.; Tong, M.-L.; Chen, X.-M. *Angew. Chem., Int. Ed.* **2002**, *41*, 1029−1031.

(24) Liu, C.-M.; Gao, S.; Kou, H.-Z. *Chem. Commun.* **2001**, 1670−1671.

DOI: 10.1021/acs.inorgchem.5b01820
Inorg. Chem. XXXX, XXX, XXX−XXX

(25) Yam, V. W. W.; Lo, K. K. W. *Chem. Soc. Rev.* **1999**, *28*, 323−334.
(26) (a) Tronic, T. A.; deKrafft, K. E.; Lim, M. J.; Ley, A. N.; Pike, R. D. *Inorg. Chem.* **2007**, *46*, 8897−8911. (b) Lim, M. J.; Murray, C. A.; Tronic, T. A.; deKrafft, K. E.; Ley, A. N.; deButts, J. C.; Pike, R. D.; Lu, H.; Patterson, H. H. *Inorg. Chem.* **2008**, *47*, 6931−6947.
(27) (a) Wang, R.; Dong, X.-Y.; Xu, H.; Pei, R.-B.; Ma, M.-L.; Zang, S.-Q.; Hou, H.-W.; Mak; Thomas, C. W. *Chem. Commun.* **2014**, *50*, 9153−9156. (b) Jayaramulu, K.; Kanoo, P.; George, S.- J.; Maji, T.-K. *Chem. Commun.* **2010**, *46*, 7906−7908.
(28) (a) Dang, S.; Ma, E.; Sun, Z. M.; Zhang, H. J. A. *J. Mater. Chem.* **2012**, *22*, 16920−16926. (b) Hou, Y.; Chen, H. H.; Yan, B. *J. Mater. Chem. A* **2014**, *2*, 13691−13697.
(29) Tang, Q.; Liu, S. X.; Liu, Y. W.; Miao, J.; Li, S. J.; Zhang, L.; Shi, Z.; Zheng, Z. P. *Inorg. Chem.* **2013**, *52*, 2799−2801.
(30) Thomas, S. W.; Joly, G. D.; Swager, T. M. *Chem. Rev.* **2007**, *107*, 1339−1386.
(31) Zou, Q.; Li, X.; Zhang, J.; Zhou, J.; Sun, B.; Tian, H. *Chem. Commun.* **2012**, *48*, 2095−2097.
(32) (a) Gupta, V. K.; Suhas. *J. Environ. Manage.* **2009**, *90*, 2313−2342. (b) Demirbas, A. *J. Hazard. Mater.* **2009**, *167*, 1−9.
(33) (a) Tsai, W.-T; Hsu, H.-C.; Su, T.-Y.; Lin, K.-Y.; Lin, C.-M.; Dai, T.-H. *J. Hazard. Mater.* **2007**, *147*, 1056−1062. (b) Wang, C.; Zhang, J.; Wang, P.; Wang, H.; Yan, H. *Desalin. Water Treat.* **2015**, *53*, 3681−3690.
(34) Allen, S.; Koumanova, B. *J. Univ. Chem. Technol. Metall.* **2005**, *40*, 175−192.
(35) (a) Rafatullah, M.; Sulaiman, O.; Hashim, R.; Ahmad, A. *J. Hazard. Mater.* **2010**, *177*, 70−80. (b) Ahmada, A.; Rafatullah, M.; Sulaiman, O.; Ibrahim, M. H.; Hashim, R. *J. Hazard. Mater.* **2009**, *170*, 357−365.
(36) (a) Jing, H.-P.; Wang, C.-C.; Zhang, Y.-W.; Wang, P.; Lia, R. *RSC Adv.* **2014**, *4*, 54454−54462. (b) Wen, T.; Zhang, D.-X.; Zhang, J. *Inorg. Chem.* **2013**, *52*, 12−14. (c) Wang, X.-L.; Luan, J.; Sui, F.-F.; Lin, H.-Y.; Liu, G.-C.; Xu, C. *Cryst. Growth Des.* **2013**, *13*, 3561−3576. (d) Hou, Y.-L.; Sun, W.-Y.; Zhou, X.-P.; Wang, J.-H.; Li, D. *Chem. Commun.* **2014**, *50*, 2295−2297.
(37) Paul, A. K.; Madras, G.; Natarajan, S. *Phys. Chem. Chem. Phys.* **2009**, *11*, 11285−11296.
(38) (a) Wang, C.-C.; Li, J.-R.; Lv, X.-L.; Zhang, Y.-Q.; Guo, G.-S. *Energy Environ. Sci.* **2014**, *7*, 2831−2867. (b) Lu, Z.-Z.; Zhang, R.; Li, Y.-Z.; Guo, Z.-J.; Zheng, H.-G. *J. Am. Chem. Soc.* **2011**, *133*, 4172−4174.

DOI: 10.1021/acs.inorgchem.5b01820
Inorg. Chem. XXXX, XXX, XXX−XXX